Room temperature variation in the threshold fields in $R_xY_{1-x}Mn_6Sn_6$ (R ≡ Ce–Nd, Sm, Gd–Ho) solid solutions

G. Venturini, R. Welter and B. Malaman

Laboratoire de Chimie du Solide Minéral, Associé au CNRS 158, Université de Nancy I, BP 239, F-54506 Vandoeuvre les Nancy Cedex (France)

Abstract

Study of the threshold field variations in $R_xY_{1-x}Mn_6Sn_6$ compounds as a function of x and R allows a relative scale of R–Mn exchange interaction strengths to be deduced. Experimental data show clearly that samarium gives rise to the strongest R–Mn interactions, followed by gadolinium, neodymium and terbium. Generally the light rare earths are more strongly coupled with Mn than the heavy ones.

1. Introduction

RMn_6X_6 (R ≡ Sc, Y, rare earth elements; X ≡ Sn, Ge) compounds exhibit a great variety of magnetic behaviour depending on the nature of the alloyed rare earth element [1–4]. All these compounds crystallize in the $HfFe_6Ge_6$- or YCo_6Ge_6-type structure [1, 2], which are respectively ordered and disordered filled derivatives of the CoSn B35 type (*P6/mmm*). The $HfFe_6Ge_6$-type structure can be described as being built of alternate (001) layers of rare earth and manganese atoms stacked along the c axis in the sequence Mn–R–Mn–Mn–R–Mn (Fig. 1), while in YCo_6Ge_6-type structure, the R atoms are randomly distributed between each Mn plane. Furthermore, in both structural types, the R atoms are located in large hexagonal RMn_{12} prisms, with R–T distances of about 3.5 and 3.3 Å for the stannide and germanide compounds respectively. Therefore, owing to the Mn atom coordination of R, these structures appear closely related to the $CaCu_5$- and $ThMn_{12}$-type structures.

Magnetic measurements on the RMn_6X_6 compounds have been widely described [1, 2]. All the studied RMn_6Sn_6 stannides [1] have the $HfFe_6Ge_6$-type structure. The (Gd–Ho)Mn_6Sn_6 compounds are ferrimagnetic, while $ErMn_6Sn_6$ is antiferromagnetic, with a metamagnetic magnetization process occurring under an applied field of 5600 Oe at room temperature, and becomes ferrimagnetic below 75 K. The (Tm,Lu,Sc,Y)Mn_6Sn_6 compounds are antiferromagnetic over the whole temperature range below T_N. In YMn_6Sn_6 ($T_N = 333$ K) a metamagnetic magnetization process probably occurs, since at room temperature the mag-
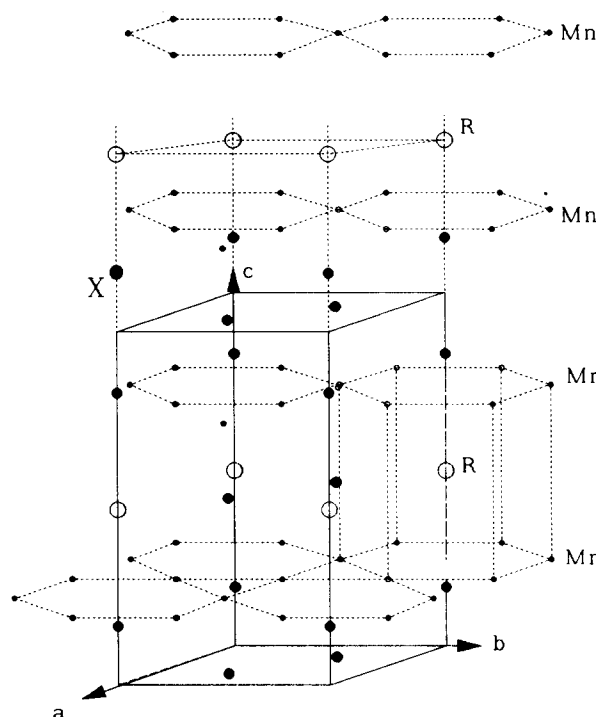

Fig. 1. $HfFe_6Ge_6$-type structure of RMn_6X_6 compounds.

netization curve begins to depart from linearity under field of about 10 kOe.

The studied RMn_6Ge_6 compounds [2] are either isotypic with the YCo_6Ge_6 (R ≡ Nd, Sm) or $HfFe_6Ge_6$ (R ≡ Sc, Y, Gd–Lu) type of structure. The light rare earths and gadolinium compounds exhibit spontaneous magnetization whereas the others are antiferromagnetic.

Neutron diffraction studies show that all these compounds are characterized by a stacking of (001) fer-

romagnetic layers of Mn or R (when paramagnetic) atoms in various coupling sequences along the c axis. $HoMn_6Sn_6$ and $TbMn_6Sn_6$ [3] exhibit a collinear ferrimagnetic arrangement due to an antiferromagnetic coupling between the R and Mn ferromagnetic sublattices, whereas in the $(Sc,Y,Er,Tm,Lu)Mn_6Sn_6$ compounds complex helical magnetic structures are observed [4]. In these latter cases further investigations are in progress.

From these studies it appears that negative magnetic interactions occur between the Mn and R (Gd, Tb, Dy, Ho) sublattices which are sufficiently strong to induce a reorientation process of the Mn sublattice, yielding ferrimagnetic arrangements. The thulium sublattice never aligns the helical Mn magnetic sublattice whereas $ErMn_6Sn_6$ has an intermediate behaviour, since the reorientation of the Mn sublattice is only observed at low temperature. Nevertheless, even at room temperature the Er–Mn magnetic coupling is significant, yielding a decrease in the threshold field from 10 kOe in YMn_6Sn_6 to 5.6 kOe in $ErMn_6Sn_6$.

A shift of the R–Mn magnetic properties is observed in the corresponding germanides. Within the heavy rare earth compounds only the gadolinium sublattice is able to align the Mn moments. The light rare earth sublattices (Nd, Sm) behave like the Gd one but $(Nd,Sm)Mn_6Ge_6$ crystallize in the disordered YCo_6Ge_6-type structure, thus preventing a fair comparison of their properties.

From these considerations we decided to investigate the $Y_{1-x}R_xMn_6Sn_6$ solid solutions by magnetization measurements in order to check the variation in the threshold fields as a function of x and the nature of the substituted R element.

Although $CeMn_6Sn_6$ and $PrMn_6Sn_6$ have not so far been identified, $NdMn_6Sn_6$ and $SmMn_6Sn_6$ are of $HoFe_6Sn_6$ [5] and YCo_6Ge_6 [6] structural types respectively [6]. Thus it appears that the stability of the $HfFe_6Ge_6$-type structure is related to the mean atomic radius (r_m) of the atoms lying on the rare earth site:

$$r_m = xr_{R^{3+}} + (1-x)r_{Y^{3+}} \leqslant 0.94 \text{ Å}$$

Under these conditions the substitution of an adequate quantity of yttrium would allow us to stabilize light rare earth (Ce–Sm) $Y_{1-x}R_xMn_6Sn_6$ solid solutions with the $HfFe_6Ge_6$-type structure. The R–Mn coupling effects on the Mn sublattice magnetic ordering in YMn_6Sn_6 can then be studied for the whole paramagnetic rare earth series, thus allowing us to deduce a relative scale of the R–Mn exchange interaction strengths in the RMn_6Sn_6 family.

2. Experimental details

All the compounds were prepared from commercially available high purity elements: Mn (powder, 99.9%),

rare earth (R) elements (ingots, 99.9%) and tin (pieces, 99.99%). Pellets of starting compositions $Y_{1-x}R_xMn_6Sn_6$ (R $\equiv$ Ce–Sm, Gd–Ho) were compacted using a steel die, annealed several times (with grinding and compacting each time) at 1073 K in sealed silica tubes under argon (0.2 atm) and finally quenched in water. At least five different compositions have been prepared in each system (see Tables 1 and 2). The purity of the

TABLE 1. Magnetic data for $R_xY_{1-x}Mn_6Sn_6$ (R $\equiv$ Ce–Sm)

$Ce_xY_{1-x}Mn_6Sn_6$

x	0.075	0.100	0.125	0.150	0.175	0.200
H_s (± 200 Oe)	4100	1800	1700	1400	1000	1000
T_N (± 2 K)	325	319	320	318	319	319

$\log(H_s)_0 = 3.82$, $A = -4.47$, $A' = -5.37$

$Pr_xY_{1-x}Mn_6Sn_6$

x	0.075	0.100	0.125	0.150	0.175	0.200
H_s (± 200 Oe)	3800	2200	2000	1400	1100	800
T_N (± 2 K)	332	330	327	326	324	323

$\log(H_s)_0 = 3.92$, $A = -5.08$, $A' = -5.25$

$Nd_xY_{1-x}Mn_6Sn_6$

x	0.050	0.075	0.100	0.125	0.150	0.175
H_s (± 200 Oe)	3800	1900	1600	1300	800	400
T_N (± 2 K)	332	330	326	325	325	324

$\log(H_s)_0 = 3.93$, $A = -6.98$, $A' = -7.42$

$Sm_xY_{1-x}Mn_6Sn_6$

x	0.035	0.050	0.080	0.100	0.125
H_s (± 200 Oe)	4500	2000	1250	1100	400
T_N (± 2 K)	333	333	331	330	331

$\log(H_s)_0 = 3.93$, $A = -10.15$, $A' = -10.24$

TABLE 2. Magnetic data for $R_xY_{1-x}Mn_6Sn_6$ (R $\equiv$ Gd–Ho)

$Gd_xY_{1-x}Mn_6Sn_6$

x	0.050	0.075	0.100	0.125	0.150
H_s (± 200 Oe)	3400	2100	800	600	200
T_N (± 2 K)	333	333	332	333	333

$\log(H_s)_0 = 4.17$, $A = -12.02$, $A' = -9.40$

$Tb_xY_{1-x}Mn_6Sn_6$

x	0.050	0.075	0.100	0.150	0.175
H_s (± 200 Oe)	4300	3100	2600	1400	900
T_N (± 2 K)	332	333	333	335	336

$\log(H_s)_0 = 3.91$, $A = -5.25$, $A' = -5.66$

$Dy_xY_{1-x}Mn_6Sn_6$

x	0.100	0.125	0.150	0.175	0.200
H_s (± 200 Oe)	4000	3600	2900	2600	2200
T_N (± 2 K)	333	332	332	331	333

$\log(H_s)_0 = 3.87$, $A = -2.64$, $A' = -3.12$

$Ho_xY_{1-x}Mn_6Sn_6$

x	0.100	0.200	0.250	0.300	0.350
H_s (± 200 Oe)	5600	3800	3200	2600	1800
T_N (± 2 K)	334	336	335	336	337

$\log(H_s)_0 = 3.95$, $A = -1.89$, $A' = -1.83$

final samples was checked by the X-ray diffraction technique using a Guinier camera (Cu $K\alpha$).

The magnetization measurements were performed between room temperature and 500 K using a Faraday balance under fields of up to 1.2 T. In order to carry out this study in the field range of the apparatus, we have considered to a first approximation that the threshold field is reached when the magnetization curve departs from linearity, i.e. when the derivate dM/dH, which is constant over the whole antiferromagnetic range, begins to increase.

$Y_{1-x}Er_xMn_6Sn_6$ and $Y_{1-x}Tm_xMn_6Sn_6$ have not been studied, since their corresponding threshold fields will not vary greatly along the solid solution. Therefore they cannot be considered as sufficiently diluted in the YMn_6Sn_6 matrix, since large values of x are necessary to ensure accurate H_s variation measurements. Moreover, according to the macroscopic properties of the corresponding $ErMn_6Sn_6$ and $TmMn_6Sn_6$ ternary stannides, they may be considered a priori as the last two members of the heavy rare earth classification (see below).

3. Results

3.1. Crystallographic data

The X-ray diffraction patterns obtained from powder samples show that all the $Y_{1-x}R_xMn_6Sn_6$ (R ≡ Ce–Sm, Gd–Ho) compounds are single-phase materials with the $HfFe_6Ge_6$-type structure, in agreement with the steric effects previously discussed (see Section 1). Furthermore, according to the small values of x (see Tables 1 and 2), the refined parameters vary slightly (by less than 0.4%) for the whole series of studied samples.

3.2. Magnetic data

The temperature dependences of the magnetization ($H_{appl} < 200$ Oe) confirm unambiguously the antiferromagnetic behaviour of all the quaternary $R_x Y_{1-x}Mn_6Sn_6$ (R ≡ Ce–Sm, Gd–Ho) solid solutions studied. The Néel temperatures, which were close to that observed in the YMn_6Sn_6 ternary compound, are given in Tables 1 and 2.

In each case a metamagnetic magnetization process is observed at room temperature. The threshold fields H_s deduced from the magnetic measurements are given in Tables 1 and 2. In all the compounds the variation in H_s with x exhibits a nearly exponential behaviour and can be fitted fairly well with a linear variation $\log(H_s) = \log(H_s)_0 + Ax$, where $\log(H_s)_0$ is the logarithm of the H_s value at $x = 0$. The values of $\log(H_s)_0$ and A for each $Y_{1-x}R_xMn_6Sn_6$ series are given in Tables 1 and 2. It appears that all the $\log(H_s)_0$ values range about the mean value $\log(H_s)_0' \approx 3.94$, which is close

to that measured in the pure YMn_6Sn_6 compound ($\log(H_s)_Y \approx 4.00$). Since the observed discrepancies may arise from experimental uncertainties, we averaged them in a second step by fitting the magnetic data assuming the same $\log(H_s)_0$ value for all the samples, i.e. $\log(H_s)_0 = 3.94$. The last refinements using the new equation $\log(H_s) = 3.94 + A'x$ lead to the A' values given in Tables 1 and 2. Figures 2 and 3 show the corresponding fitted curves for the light and heavy rare earth $Y_{1-x}R_xMn_6Sn_6$ solid solutions respectively.

4. Discussion

The experimental value of A' deduced from threshold field variations in the $R_xY_{1-x}Mn_6Sn_6$ solid solutions may constitute a new approach to the ambiguous problem of the R–T exchange interactions in intermetallic
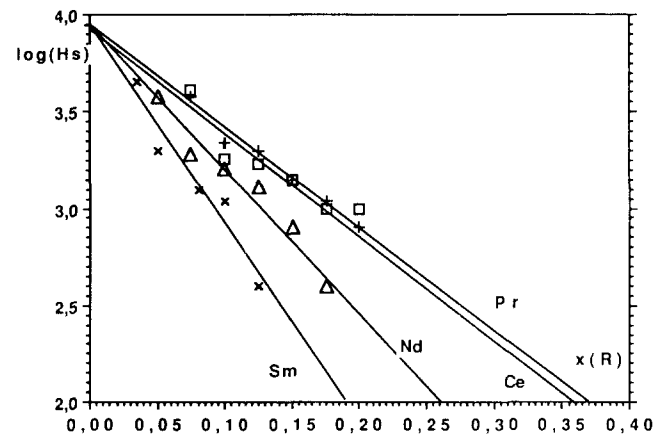

Fig. 2. Dependence on x of the logarithm of the threshold field H_s for light rare earth compounds. The solid lines correspond to the fits.
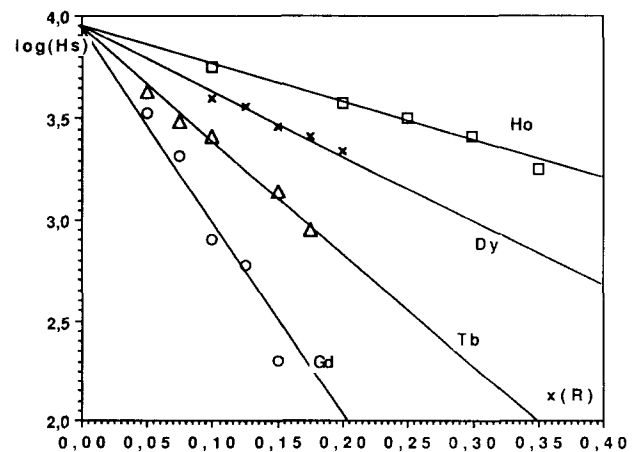

Fig. 3. Dependence on x of the logarithm of the threshold field H_s for heavy rare earth compounds. The solid lines correspond to the fits.

compounds which has been discussed in several reports on rare-earth-based supermagnets [7, 8]. Thus the RMn_6Sn_6 compounds are a nice testing ground for the study of the rare earth-transition metal magnetic interactions.

First, it is worthwhile to note the close correlations between the A' values and the macroscopic magnetic properties of RMn_6X_6 ($R \equiv Ge, Sn$) compounds. In each series an antiferromagnetic behaviour is found with rare earth elements for which the lower A' values are observed, while a ferri- or ferromagnetic behaviour occurs with those corresponding to the higher A' values.

The study of $R_xY_{1-x}Mn_6Sn_6$ solid solutions with a small percentage of substituted paramagnetic R element allows us to investigate the effect of the R–Mn interactions only. The R–R interactions may be considered as negligible since they are generally dominated by the T–T and R–T interactions in intermetallic compounds and in the present compounds are smoothed even more by the dilution of the paramagnetic element in the yttrium sublattice. Since the introduction of small quantities of R element in the YMn_6Sn_6 matrix does not greatly change the cell parameters and volumes, the Mn–Mn interactions may be considered to a first approximation as being constant in all the studied compounds. Formally, they vary slightly in the studied range, since a decrease (less than 4%) in the T_N values is observed (Tables 1 and 2). Complementary studies on $R_xY_{1-x-y}Lu_yMn_6Sn_6$ solid solutions (with y chosen so as to keep the cell volume constant) would allow us to smooth this effect. Such studies are under way. Nevertheless, in the present study it is reasonable to consider that the different H_s values measured indirectly reflect the competition between the quite constant interlayer Mn–Mn interactions yielding the helical arrangement observed in YMn_6Sn_6 and the negative (or positive) R–Mn couplings which lead to the reorientation process of the Mn sublattice, giving rise e.g. to the ferrimagnetic structures determined for $HoMn_6Sn_6$ and $TbMn_6Sn_6$ [3].

The close correlations between the experimental A' values and the De Gennes factors are shown in Fig. 4. This close correlation is especially evident in the case of the heavy rare earths. As already remarked by several authors, the Mn–light rare earth magnetic interactions are larger than expected [9]. This effect has been attributed to the larger exchange interaction between 4f and 5d electrons in the light rare earths resulting from the decrease in the spatial extent of the 4f shell with the rare earth atomic number. Similarly, the large experimental A' value observed for cerium,
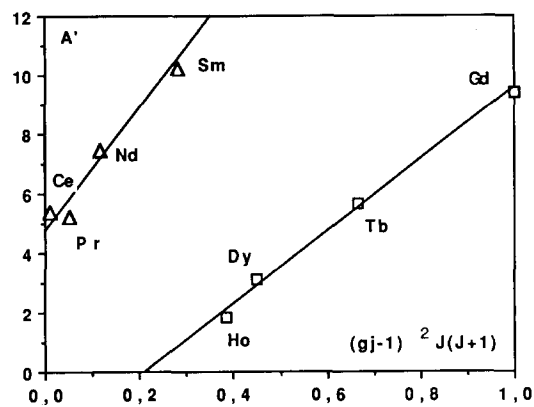

Fig. 4. Plot of calculated A' values *vs.* the De Gennes factor.

close to that of praseodymium, may be correlated with a particular hybridization of the Ce 4f state.

In conclusion, the relative scale of the R–Mn exchange interaction strengths deduced from magnetization measurements may constitute a guideline in the search for rare-earth-based compounds with hard magnetic properties. Since the rare earth element involved in these compounds must have a large absolute value of the Stevens coefficient and a strong R–T coupling, the best candidate should be samarium, followed by neodymium and then prasedymium which have A' values close to that of terbium but have larger Stevens coefficients.

Finally, it is necessary to determine the sign of the R–Mn interaction in the light rare earth RMn_6X_6 systems. In order to investigate this important point, neutron diffraction studies of $Pr_{0.4}Y_{0.6}Mn_6Sn_6$ (Hf-Fe$_6$Ge$_6$-type) and $NdMn_6Ge_6$ (YCo$_6$Ge$_6$-type) compounds are in progress.

References

1 G. Venturini, B. Chafik El Idrissi and B. Malaman, *J. Magn. Magn. Mater.*, 94 (1991) 35.
2 G. Venturini, R. Welter and B. Malaman, *J. Alloys Comp.*, 185 (1992) 99.
3 B. Chafik El Idrissi, G. Venturini, B. Malaman and D. Fruchart, *J. Less-Common Met.*, 175 (1991) 143.
4 G. Venturini, B. Chafik El Idrissi and B. Malaman, unpublished results, 1993.
5 B. Chafik El Idrissi, G. Venturini and B. Malaman, *Mater. Res. Bull.*, 26 (1991) 1331.
6 G. Venturini, R. Welter and B. Malaman, unpublished results, 1993.
7 K. H. J. Buschow, *Rep. Prog. Phys.*, 1991, p. 1123.
8 J. J. M. Franse and R. J. Radwanski, Crystal-field and exchange interactions in hard magnetic materials, *Proc. NATO Advanced Study Institute on Supermagnets, Hard Magnetic Materials, Il Ciocco, June 1990*, Kluwer, Dordrecht, 1991, p. 119.
9 E. Belorisky, M. A. Fremy, J. P. Gavigan, D. Givord and H. S. Li, *J. Appl. Phys.*, 61 (1987) 3971.